Smectic bubble lasers for acoustic and pressure measurements in air and water

Zala Korenjak [1,2] and Matjaž Humar [1,2,3,*]

[1] *Condensed Matter Department, Jožef Stefan Institute, Jamova 39, 1000 Ljubljana, Slovenia*
[2] *Faculty of Mathematics and Physics, University of Ljubljana, Jadranska 19, 1000 Ljubljana, Slovenia*
[3] *CENN Nanocenter, Jamova 39, 1000 Ljubljana, Slovenia*

(Received 14 March 2025; revised 15 July 2025; accepted 11 August 2025; published 8 September 2025)

Recently, we have demonstrated that dye-doped soap and smectic bubbles can be used as lasers. Here we investigated smectic bubble lasers for their potential to measure pressure changes in both air and water and as microphones. Smectic bubbles consist of a very thin smectic liquid crystal film. In contrast to ordinary soap bubbles, smectic bubbles are highly stable. When illuminated with a pump laser, they exhibit whispering gallery mode lasing with sharp, regularly spaced peaks in the emission spectrum. The bubbles enable extremely precise measurement of pressure changes based on wavelength shifts of the lasing peaks. We have demonstrated that smectic bubbles can be inflated under water and used as water pressure sensors. Additionally, we have used smectic bubble lasers in air as highly sensitive microphones to detect sound waves across different frequencies with advantages over conventional microphones. Their extremely thin walls result in negligible acoustic impedance. Furthermore, bubble size changes due to pressure variations depend only on bubble volume, eliminating the need for calibration and making performance independent of manufacturing precision or defects. This also leads to a linear amplitude response, and a flat frequency response over a wide range of frequencies. Unlike most microphones, bubble lasers can measure arbitrarily small frequencies down to static pressure, making them promising candidates for acoustic wave detection in various applications.

DOI: 10.1103/p1mc-1gp6

I. INTRODUCTION

A smectic bubble consists of a thin smectic liquid crystal film that is inflated into a spherical shape [1,2]. Unlike a regular soap bubble made of a soap-water mixture, a smectic bubble is composed exclusively of smectic liquid crystals. These molecules form well-defined layers, which give the bubble unique properties. The thickness of the bubble can be uniform, even down to individual molecular layers, and remains highly stable despite a significant size-to-thickness ratio. This stability allows the bubble to last indefinitely as long as the internal air volume is kept constant.

Different aspects of smectic bubbles have been studied, including surface tension [3,4], gas permeation through a smectic film [5], collapse dynamics [6], and dynamics of free-floating smectic bubbles [7–9]. Recently, we showed that dye-doped smectic bubbles can support whispering gallery mode (WGM) lasing [10]. Optical resonances, known as WGMs, occur when light is trapped in a spherical object due to multiple total internal reflections and circulates near the surface of the sphere. Thin smectic bubble lasers have been shown to support only a single set of optical modes (first radial mode and one polarization), resulting in a frequency-comb-like emission spectrum with hundreds of regularly spaced peaks. The lasing makes it possible to measure extremely small changes in the size of the bubble, which enables sensing of static electric field and pressure with extremely high sensitivity, resolution, and dynamic range.

Since smectic bubbles are soft and very light due to their extremely small thickness, they should also be sensitive to fast pressure changes and, therefore, sound. Since smectic bubble lasers can also measure static pressure, they could offer a unique platform with a very wide frequency response, including infrasound. The detection of low-frequency acoustic signals is important for many applications, such as gas sensing with photoacoustic detection [11], health monitoring [12], and natural disaster monitoring [13]. Conventional miniature microphones (such as microelectromechanical systems or fiber optic acoustic sensors) have some disadvantages; for example, limited

*Contact author: matjaz.humar@ijs.si

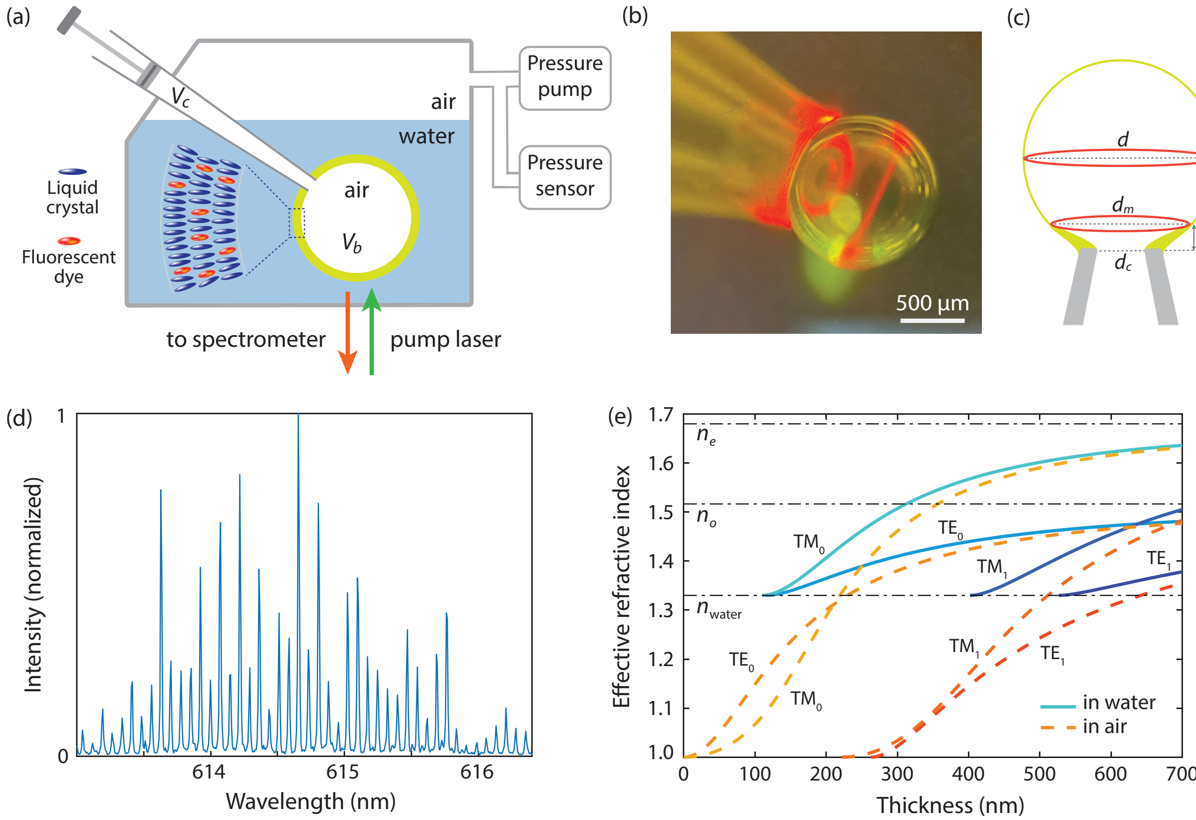

FIG. 1. Smectic bubble lasers under water. (a) Experimental setup for studying smectic bubbles under water. (b) Image of a lasing smectic bubble under water. The edge of the bubble was illuminated with a pump laser. The laser light is generated in two planes simultaneously, in the center of the bubble and at the meniscus, and can be seen as two bright red rings. (c) Sketch of two possible planes of WGM circulation in the smectic bubble, in the middle of the bubble and at the upper end of the meniscus. (d) Typical spectrum of a lasing smectic bubble. (e) Effective refractive indices for different modes calculated for a slab liquid crystal waveguide with one side air and the other water (solid line) and air (dashed line) for light with a wavelength of 600 nm.

sensitivity at low frequencies, nonflat frequency response, and complicated manufacturing.

Here we first demonstrate the stability and performance of the smectic bubble laser under water and the ability to measure pressure changes in water. Then the use of smectic bubble lasers as microphones is reported.

II. RESULTS

A. Smectic bubbles under water

To make smectic bubbles, 4′-octyl-4-biphenylcarbo nitrile (8CB) liquid crystal, which is in the smectic-A phase at room temperature, doped with 0.2% Pyrromethene 597 (Exiton) was used. Plastic pipette tips (Eppendorf) with a built-in piston (0.1 ml) were used as capillaries to inflate the bubbles. The capillary was dipped into the liquid crystal so that a small amount entered the capillary. To make smectic bubbles under water, a small transparent plastic container was half filled with deionized water and the tip of the capillary was immersed in the water to a depth of a few millimeters. When the capillary was under water, the air pressure in the capillary was slowly increased by our pushing the piston by hand to inflate a millimeter-sized bubble [Fig. 1(a)]. If the bubble was inflated in air and then immersed in water, it burst immediately. The thickness of the smectic layer between the air inside and the water outside the bubble cannot be precisely controlled, but it appears to be mostly uniform with occasional smectic islands (regions of higher thickness) [2,8]. The image of a bubble in between crossed polarizers indicates a uniform radial orientation of the molecules, the same as in smectic bubbles in air. On the basis of the interference colors observed in the reflected light, the thickness of the smectic film was typically in the range from 100 to 3000 nm.

To generate laser light, the smectic bubbles were illuminated at an edge with a nanosecond pulsed optical parametric oscillator (Opotek, Opolette 355) at 532 nm and a repetition rate of 20 Hz and observed with an inverted microscope (Nikon Ti2) through a 4×, 0.13 numerical aperture objective. The emitted laser light was visible as a bright red ring due to the circulation of the WGMs

[Fig. 1(b)]. Typical threshold values for pulse power were on the order of a few microjoules, similar to those of smectic bubbles in air. Depending on the position of the pump laser beam, the WGMs can circulate in the central plane of the bubble or near the capillary [Figs. 1(b) and 1(c)]. Where the bubble is attached to the capillary, a thicker liquid crystal meniscus is formed [6]. WGMs can circulate at the upper end of the meniscus, at the boundary with the rest of the bubble with uniform thickness. Lasing at the meniscus tends to be stabler and exhibits greater intensity. Both lasing in the center and lasing at the meniscus were used in experiments.

The spectrum of the emitted light was captured by a high-resolution spectrometer (Andor Shamrock SR-500i) with 0.007 nm spectral resolution. The spectrum contained uniformly distributed, sharp lasing peaks [Fig. 1(d)]. The WGM resonance condition can be approximated as $2\pi r n_{\text{eff}} = \lambda l$, where r is the radius of the bubble, λ is the wavelength of the mode, l is the azimuthal mode number, and n_{eff} is the effective refractive index. The effective refractive indices were calculated with standard equations for light propagation in a flat slab waveguide [14]. The slab is a birefringent smectic liquid crystal film with two different bulk refractive indices for TE and TM modes ($n_o = 1.51$ and $n_e = 1.68$, respectively). On one side is air ($n = 1$) and on the other side is water ($n = 1.33$).

The minimum thickness of a smectic film with one side in water supporting the propagation of light is approximately 100 nm [Fig. 1(e)]. For smectic bubbles in air, there is no minimum thickness for light propagation. In water at thicknesses greater than the minimum thickness, the TE_0 and TM_0 modes are both allowed. Since the effective refractive index of the TM_0 mode is significantly greater than that of the TE_0 mode, this is the only mode lasing, which was confirmed by our measuring the emission intensity through a polarizer. For a smectic bubble with a diameter of 1.2 mm, the free spectral range of the lasing modes is 0.073 nm [Fig. 1(d)]. This results in an effective refractive index of 1.4, corresponding to an approximate thickness of 200 nm, for TM polarization.

Similarly to smectic bubble lasers as pressure sensors in air [10], we tested the performance of smectic bubble lasers as pressure sensors under water. The pressure in the air above the water in which the bubble was placed was changed in a controlled manner with the use of a pressure controller (Elveflow, OB1, 0–20 kPa) and was monitored with an additional pressure sensor [Fig. 1(a)]. When we increased the pressure in air, the pressure inside the bubble also increased. The small change in the volume of the bubble corresponds to the adiabatic contraction due to the change in pressure and depends on the initial volume of the bubble V_b and the additional volume of air in the capillary V_c to which the bubble is attached. Because of Laplace's law, it generally also depends on the surface tension, but with a sufficiently small volume of air in the capillary (in our case $V_c/V_b + 1 \approx 40$), the surface tension term is negligible [10], so the small relative change in size for an adiabatic case is expressed as

$$\frac{\Delta d}{d} = -\frac{\Delta p}{3\kappa p_0}(V_c/V_b + 1), \tag{1}$$

where p_0 is the atmospheric pressure, $\kappa = 7/5$ is the heat capacity ratio, and Δp the small change in pressure. We measured the relative changes in the size of the bubble due to pressure by measuring the shifts of the lasing peaks. Without application of any pressure change, the spectrum was very stable in time, meaning that any changes in the spectrum corresponded to a change in size due to pressure. Measuring the spectrum of the emitted light of a 1.2 mm bubble over time without applying pressure, we found that the wavelength shift of the lasing peaks was only 0.004 nm/s toward longer wavelengths [Fig. 2(a)]. The noise in the position of the peaks over time was 0.025 nm. Since the relative size change corresponds approximately to the relative wavelength shift ($\Delta d/d = \Delta\lambda/\lambda$), this means that the diameter of the smectic bubble increases with a very small rate of 8 nm/s. This is an advantage over smectic bubbles in air, where the diameter change rate was 1.1 μm/s for a 1.9 mm bubble due to the diffusion of air molecules through the thin film [5,10]. When we applied a slowly varying pressure with a rate of 32 Pa/s, there were visible changes in the spectrum over time. The peaks shifted to shorter wavelengths [Fig. 2(b)] as the bubble shrank with increasing pressure, and as the pressure decreased, the wavelengths of the peaks returned to longer wavelengths [Fig. 2(c)]. The wavelengths of lasing peaks were fitted from each spectrum in time. At some times there was loss of the signal from certain azimuthal lasing modes, resulting in a gap in the spectrum, as seen in Fig. 2(c). This is probably due to the oscillations of the bubble size and smectic islands that can appear on the bubble. Despite this, at any time there are at least a few peaks lasing, so at each time step, we calculated the average shift of all peaks, which in this case was smaller than the distance between two peaks (free spectral range) due to the small rate of change. The average rate of peak wavelength shift was 0.12 nm/s for both decreasing size and increasing size. If we want to determine the change in the size of the bubble, the relative wavelength shift $\Delta\lambda/\lambda$ is more relevant, so we measured the average relative shift of the peaks at each time step. The collective response of the relative wavelength shift was calculated as the cumulative sum of the wavelength shifts at each time step. The relative shift of the lasing peaks with an amplitude of $(1.8 \pm 0.2) \times 10^{-3}$ followed well the applied pressure, which was periodically varied with a triangular waveform with an amplitude of 320 Pa and a period of 20 s [Fig. 2(d)]. The diameter d of the smectic bubble measured from the image was 1.2 mm.

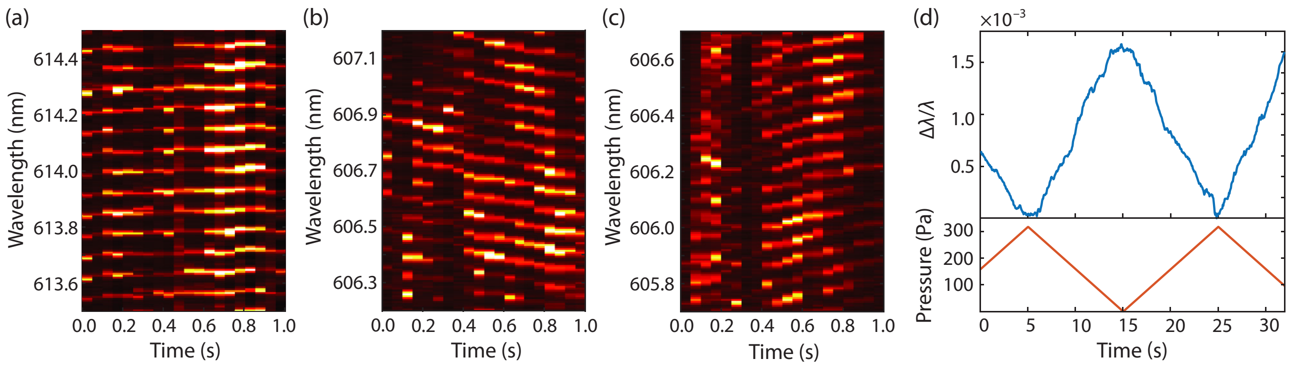

FIG. 2. Pressure measurement with smectic bubble lasers under water. (a) Lasing spectrum of a 1.2 mm smectic bubble under water in time. The color represents the intensity. (b) Lasing spectrum in time when the pressure around the bubble was varied. Lasing peaks shifted to shorter wavelengths as the pressure was increased with a rate of 32 Pa/s. (c) Lasing peaks shifted to longer wavelengths as the pressure was decreased. (d) Relative shift of the lasing peaks in time of a smectic bubble, measured by following the lasing peaks as the applied pressure was slowly varied between 0 and 320 Pa.

The WGMs were generated at the meniscus with diameter $d_m = 1.0$ mm, which was located $h = (70 \pm 30)$ μm above the capillary (diameter $d_c = 0.9$ mm) [Fig. 1(c)]. The change in the meniscus diameter, calculated from the relative wavelength shift, $\Delta d_m = d_m \times \Delta\lambda/\lambda = 2.2$ μm. The calculated size change Δd of the bubble obtained withEq. (1) due to the applied pressure is 30 μm. The change in the diameter of the meniscus is related to the size change of the whole bubble as

$$\frac{\Delta d_m}{\Delta d} = \frac{2dh}{d_m\sqrt{d^2 - d_c^2}}. \qquad (2)$$

The corresponding change in the diameter of the meniscus Δd_m calculated by this equation is (6 ± 2.5) μm, which roughly agrees with the size change calculated from the wavelength shift. The large error is primarily due to uncertainty in determining h and V_c.

B. Sound measurements with smectic bubble lasers

To measure sound, smectic bubble lasers in air were used. The procedure for inflating smectic bubbles was the same as in water, except the bubbles were produced in air. The smectic bubbles were placed in a transparent plastic container to minimize air currents that could affect the size or shape of the smectic bubbles. To apply sound, a speaker was placed outside the plastic container, approximately 15 cm from the bubble [Fig. 3(a)]. Small holes were drilled into the container so that sound pressure waves could reach the bubble. The amplitude and frequency of the sound were controlled by a function generator. A sinusoidal signal with a single frequency or a combination of different frequencies from 20 to 200 Hz was used. The lowest frequency was limited by the performance of the speaker and the noise in the environment, and the highest frequency was limited by the maximum frame acquisition rate of the spectrometer (500 Hz). Acoustic pressure was in the range from 30.5 to 82 mPa (63.7–72.3 dB), measured with a sound meter and a calibration microphone (Beyerdynamic MM1) placed inside the container at the location of the bubble. The amplitude of the noise in the environment was between 0.4 and (16 ± 3) mPa in the frequency range between 20 and 200 Hz, measured inside the plastic container at the location of the smectic bubble.

To observe the laser light, the smectic bubbles were pumped with a pulsed laser (Ekspla NT242) at 532 nm and a repetition rate of 500 Hz. With high enough repetition rate of the spectrometer, we were able to observe temporal oscillations in the wavelengths of lasing peaks [Fig. 3(b)], which are the result of the size oscillation of the smectic bubble. The spectra were collected for 6–7.5 s. In contrast to the smectic bubbles under water, the diffusion of air through the smectic film in air is considerable. Therefore, the size of the bubble slowly decreases over time, and in addition to the oscillations, the wavelengths of the peaks slowly shift to shorter wavelengths.

To get information about the frequency, phase, and amplitude of the sound, we analyzed the peak oscillations in the spectrum in time. Shifts of lasing peaks were fitted in the same manner as for pressure measurements under water. To get the frequency spectrum of the bubble size change rate $\Delta d/\Delta t$, we performed a Fourier transformation of the rate of peak wavelength shifts in time. For the applied sound with a frequency of 80 Hz and acoustic pressure amplitude of 61.5 mPa, there is a well-distinguished peak at the frequency of the sound used [Fig. 3(c)]. For the bubble with a diameter of 1.2 mm, the amplitude of the bubble size change rate oscillations at the sound frequency was 500 μm/s. Background noise is small up to zero frequency, where there is a narrow peak due to constant shrinkage of the bubble size. The peak at the sound frequency was narrow with FWHM of 0.3 Hz. Since we measure the rate of the relative wavelength shift, we have

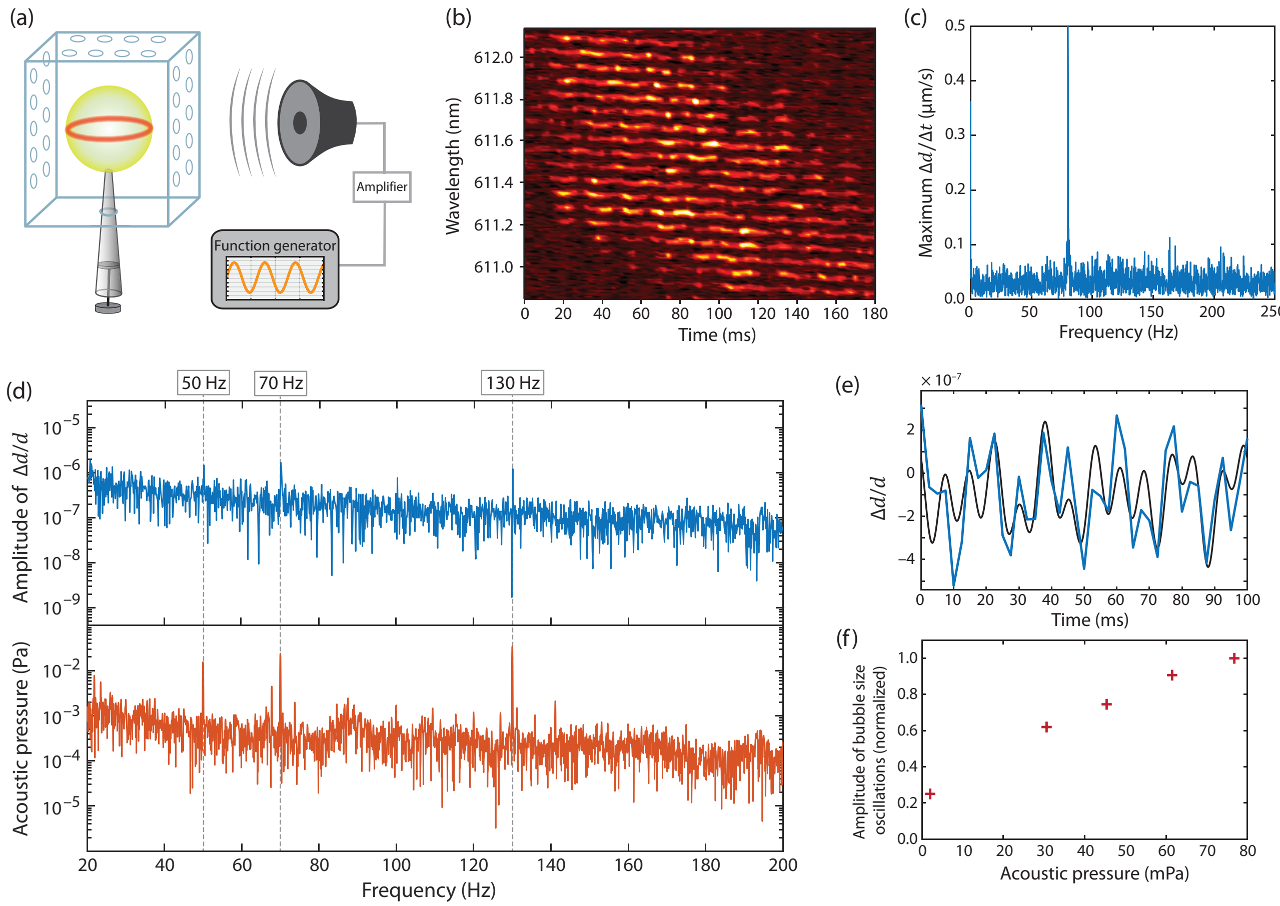

FIG. 3. Sound measurements with smectic bubble lasers. (a) Experimental setup for sound measurements with smectic bubble lasers. A bubble is pumped with a pulsed laser, and the resulting laser light is sent to the spectrometer. (b) The lasing spectrum of a 1.6 mm smectic bubble in time when sound with a frequency of 50 Hz and acoustic pressure of 82 mPa was applied. Oscillations of spectral peaks are clearly visible. (c) The frequency spectrum in terms of maximum bubble size change rate $\Delta d/\Delta t$ is calculated as the Fourier transformation of the rate of lasing peak shifts over time. The acoustic pressure of sound used was 61.5 mPa and the frequency was 80 Hz. (d) Measured sound spectra when sound with three different frequencies is applied: 50, 70, and 130 Hz. The top graph shows the spectrum of the amplitude of relative bubble size oscillations calculated with the Fourier transformation of lasing peak shifts. The bottom graph shows the sound spectrum of the same signal in terms of acoustic pressure measured with the calibration microphone. (e) Relative bubble size change in time (blue) calculated with inverse Fourier transformation from the filtered sound spectrum in (d) and the fitted function used on the speaker to make sound (black). (f) Normalized amplitude of bubble size oscillations at different acoustic pressures for sound with a frequency of 80 Hz.

to divide the Fourier transform of the rate by frequency to get the spectrum of the relative wavelength shift $\Delta\lambda/\lambda$. In addition to sound with a single frequency, we also measured sound with a mixture of sinusoid tones with different frequencies and phases. Figure 3(d) shows the sound spectrum of the signal with three different frequencies of 50, 70, and 130 Hz. It was measured as the amplitude of the relative wavelength shifts, which equals the relative diameter shifts of the bubble. The spectrum obtained from the smectic bubble laser is compared with the sound spectrum measured with a calibration microphone in terms of acoustic pressure. The two spectra match well for all three indicated frequencies of the sound used. The flat background sound with some additional frequencies present (e.g., 100 and 175 Hz) also matches well with the calibration microphone. This indicates that the frequency response of the smectic bubble laser in this frequency region is flat.

Moreover, by making an inverse Fourier transformation of the signal in the 1.5 Hz band around the peaks in the sound spectrum, we obtained the shape of the original signal applied to the speakers, which in addition to the amplitude contains information about the phase of each frequency component. In Fig. 3(e), there is a comparison of the filtered inverse Fourier transform of relative bubble size oscillations and the fitted function that was used to generate sound. This means that we can actually reproduce, or in other words play back, the original sound.

In the approximation of small pressure amplitude, the change in bubble size is approximately linearly proportional to the pressure change [Eq. (1)]. To check the linearity, we used sound with 80 Hz and acoustic pressures between 30.5 and 77 mPa. We calculated the area under the peak in the frequency spectrum as the sum of all values in the 5 Hz band around the peak. The resulting normalized amplitude of bubble size oscillations versus acoustic pressure is shown in Fig. 3(f). The lowest point in this graph corresponds to the amplitude of the background noise, measured with the lasing spectra without applied sound. In the measured pressure range, the response is close to linear. At much higher pressures, the saturation would occur according to the equation that relates the change in external pressure to the change in bubble size without the approximation of small pressure amplitude [10].

III. CONCLUSION

In conclusion, we have demonstrated the use of smectic bubble lasers under water to measure small pressure changes and the use of smectic bubble lasers in air as microphones. Smectic bubbles are even more stable in water than in air. This is mainly due to negligible leakage of air through the thin smectic film, which causes the size of the bubble to slowly decrease over time in the case of bubbles in air. For both smectic bubbles in air and smectic bubbles in water, only a single set of optical modes propagates at typical thicknesses of smectic bubbles, resulting in a lasing spectrum with regularly distributed laser peaks.

Compared with other microphones of similar size, smectic bubble lasers are very easy to form, not requiring any complicated manufacturing procedures. The small thickness of the smectic film results in a very low weight of the bubble. This yields small acoustic impedance, which is important so that the microphone does not affect the sound field it measures. The frequency of sound with a wavelength comparable to the size of a smectic bubble is a few hundred kilohertz. Although the lowest nonradial resonant frequency of the smectic bubbles used in the experiments is lower than this, it should not be important, as at wavelengths longer than the bubble, the bubble will experience mainly isotropic pressure changes, which are unlikely to excite nonradial (quadrupole, octupole, etc.) resonant oscillations. Therefore, a relatively flat frequency response is expected up to frequencies well above audible sound. Still, this should be confirmed experimentally. Also, the bubble is not isolated from the capillary, which may affect the frequency response. The length of each measured pulse is short enough (a few nanoseconds) for a sampling rate of up to a few hundred megahertz. The smallest acoustic pressure we detected with the smectic bubble laser, limited by the background noise, was 0.5 mPa (28 dB) as measured with a calibration microphone at a frequency of around 180 Hz. The optically limited minimum measurable sound pressure may be even lower, especially if a larger volume of air in the capillary is used [10]. The signal of the smectic bubble microphone is linearly proportional to the sound pressure in the measured range of acoustic pressures. Although we showed microphone operation down to 20 Hz, due to the limitations in sound production and reference measurement, smectic bubble lasers in principle can measure even lower frequencies, all the way down to 0 Hz, which was shown with static pressure measurements [10]. Very few other typical microphones can measure both static pressure and sound with high frequencies. An alternative commercial instrument would be a capacitance diaphragm manometer (Baratron), which can measure differential pressures up to 13.3 Pa with a resolution of 0.01 mPa and an accuracy of around 10 mPa and has an integration time short enough to measure sound from static pressure up to a frequency of 1 kHz. Despite this, smectic bubble lasers are much smaller (millimeter size compared with centimeter size of the manometer) and lighter, meaning they disturb the sound field much less. In addition, the dynamic range of pressures measurable with smectic bubble lasers is approximately 10^5 and the pressure range can be tuned with additional volume in the capillary. Lastly, smectic bubble microphones may also be used under water, which we have already indicated using bubbles as sensors of slowly changing pressure under water.

ACKNOWLEDGMENTS

This project has received funding from the European Research Council under the European Union's Horizon 2020 research and innovation programme (Grant Agreement No. 851143) and from the Slovenian Research Agency (ARRS) (Grants No. N1-0362 and No. P1-0099).

DATA AVAILABILITY

The data that support the findings of this article are openly available [15].

[1] P. Oswald, Dynamics of collapse of a smectic bubble, J. Phys. **48**, 897 (1987).

[2] R. Stannarius and C. Cramer, Self-supporting bubbles of thermotropic smectic liquid crystals, Europhys. Lett. **42**, 43 (1998).

[3] R. Stannarius, C. Cramer, and H. Schüring, Self-supporting smectic bubbles, Mol. Cryst. Liq. Cryst. Sci. Technol., Sect. A **329**, 423 (1999).

[4] H. Schüring, C. Thieme, and R. Stannarius, Surface tensions of smectic liquid crystals, Liq. Cryst. **28**, 241 (2001).

[5] Y. Ishii and Y. Tabe, Gas permeation of LC films observed by smectic bubble expansion, Eur. Phys. J. E **30**, 257 (2009).

[6] F. Caillier and P. Oswald, Collapse dynamics of smectic-A bubbles, Eur. Phys. J. E **20**, 159 (2006).

[7] Kathrin May, Kirsten Harth, Torsten Trittel, and Ralf Stannarius, Dynamics of freely floating smectic bubbles, Europhys. Lett. **100**, 16003 (2012).

[8] Noel A. Clark, Alexey Eremin, Matthew A. Glaser, Nancy Hall, Kirsten Harth, Christoph Klopp, Joseph E. Maclennan, Cheol S. Park, Ralf Stannarius, Padetha Tin, William N. Thurmes, and Torsten Trittel, Realization of hydrodynamic experiments on quasi-2D liquid crystal films in microgravity, Adv. Space Res. **60**, 737 (2017).

[9] Patricia Dähmlow, Torsten Trittel, Kathrin May, Kirsten Harth, and Ralf Stannarius, Surface reduction of freely floating smectic bubbles, Liq. Cryst. **45**, 993 (2018).

[10] Zala Korenjak and Matjaž Humar, Smectic and soap bubble optofluidic lasers, Phys. Rev. X **14**, 011002 (2024).

[11] Dakshith Ruvin Wijesinghe, Md Abu Zobair, and Mina Esmaeelpour, A review on photoacoustic spectroscopy techniques for gas sensing, Sensors **24**, 6577 (2024).

[12] Yuki Okamoto, Thanh-Vinh Nguyen, Hidetoshi Takahashi, Yusuke Takei, Hironao Okada, and Masaaki Ichiki, Highly sensitive low-frequency-detectable acoustic sensor using a piezoresistive cantilever for health monitoring applications, Sci. Rep. **13**, 6503 (2023).

[13] Jeffrey Bruce Johnson and Maurizio Ripepe, Volcano infrasound: A review, J. Volcanol. Geotherm. Res. **206**, 61 (2011).

[14] Kenji Kawano and Tsutomu Kitoh, *Introduction to Optical Waveguide Analysis: Solving Maxwell's Equation and the Schrödinger Equation* (John Wiley & Sons, New York, 2004).

[15] https://doi.org/10.5281/zenodo.15878963.